SEAGULL™ VARIABLE ANGLE REFLECTION ACCESSORY **NO. 60501**

Near Critical Angle FTIR ATR Spectroscopy With a Variable Angle Reflection Accessory

JOSEPH P. LUCANIA AND S. L. BERETS
HARRICK SCIENTIFIC PRODUCTS, INC., BOX 277, PLEASANTVILLE, NY 10570

POSTER PAPER NO. 1870-9P, SPECTROSCOPY: IR, NEAR IR AND RAMAN, PRESENTED AT THE 2006 PITTSBURGH CONFERENCE, ORANGE COUNTY CONVENTION CENTER, ORLANDO, FL, MARCH 15, 2006

OBJECTIVE

Variable angle ATR FTIR spectroscopy is used to study the effect on sensitivity of changing the angle of incidence. The angle of incidence can be decreased (moved closer to the critical angle) in order to increase sensitivity. As the critical angle is approached, however, spectral distortion results. Such distortion can be offset by the use of an aperture. Conversely, the angle of incidence can be increased to reduce sensitivity in cases where absorbance values are too high.

ABSTRACT

Although ATR spectroscopy near the critical angle seems to offer the advantage of heightened sensitivity, it is a technique that is generally eschewed by scientists and accessory manufacturers. Most organic compounds have a bulk refractive index of approximately 1.5. For the most common ATR element material, Zinc Selenide, with a refractive index of 2.42, the critical angle is 38 degrees. At smaller angles, total internal reflection no longer occurs. Furthermore, as one approaches the critical angle, spectral distortion results. This is due to fluctuations in the refractive index around absorbance maxima in the analyzed compound and to the beam spread in modern FTIR instrumentation. Most fixed angle ATR accessory designs protect against such phenomena by using an angle of incidence of 45 degrees, safely higher than the critical angle for most samples. In some cases, a larger angle or a higher refractive

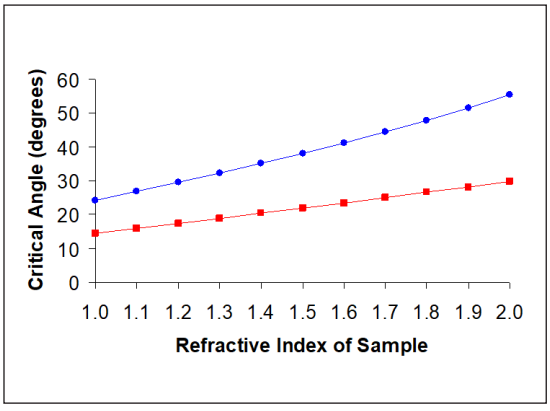

Figure 1. Critical angle vs. refractive index of sample for Zinc Selenide (blue) and Germanium (red).

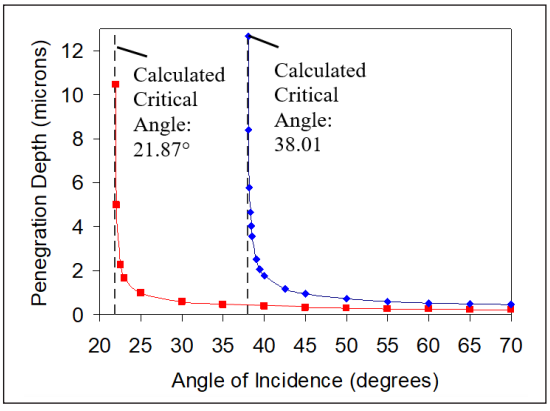

Figure 2. Penetration depth vs. angle of incidence for Zinc Selenide (blue) and Germanium (red).

Figure 3. SeagullTM variable angle reflection accessory with ATR kit and liquid cell installed.

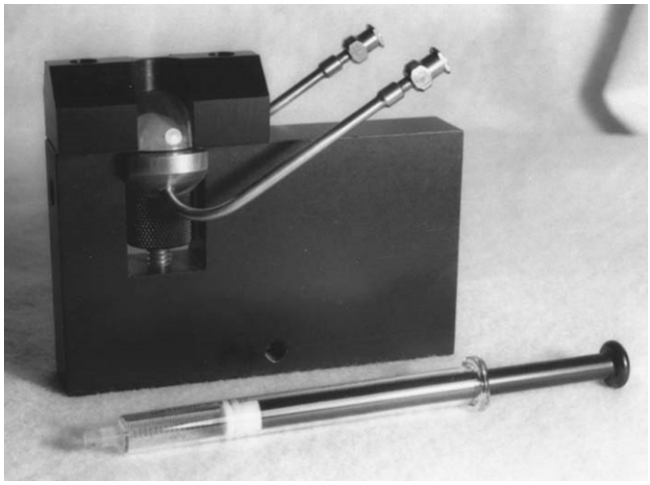

Figure 4. SeagullTM Zinc Selenide ATR kit with liquid cell and Luer-tipped syringe.

index ATR material is recommended, especially for use with intensely absorbing samples, to further reduce any distortion. Despite such conderations, there remains the possibility of hypersensitive analysis in the 45 to 38 degree regime. For it is here that the effective pathlength of ATR spectroscopy increases dramatically. To investigate this potential, the Harrick Scientific Products variable angle reflection accessory, the Seagull™, equipped with a ZnSe ATR element and a liquid cell, is employed. Examples of advantages and pitfalls will be given and the use of apertures will be discussed.

INTRODUCTION

Critical Angle

In an ATR configuration, light traveling within the ATR element reaches the interface between the element and sample. (The refractive index of the ATR element is generally much higher than the sample.) The angle of incidence for which the refracted ray emerges tangent to the surface of the element is called the critical angle, A_c.[1] Derived from Snell's Law, Ac is given by

$$A_c = \sin^{-1} (n_2/n_1) \qquad (1)$$

where n_1 is the refractive index of the ATR element and n_2 is the refractive index of the sample. At angles greater than A_c, light interacts with the sample and is reflected back into the ATR element at the same angle as the incident angle. At angles less than A_c, light exits the ATR element and cannot be collected by the detector of the spectrometer.

Figure 1 plots the critical angle for two common ATR element materials, Zinc Selenide (ZnSe), the material used in this study, and Germanium (Ge) versus the refractive index of the sample. The graph begins at the refractive index of air, 1.00. Most organic and inorganic (e.g., aqueous) substances analyzed with ATR spectroscopy have a refractive index between 1.3 and 1.7. In the calculations for Figure 1, the refractive indices of the two materials

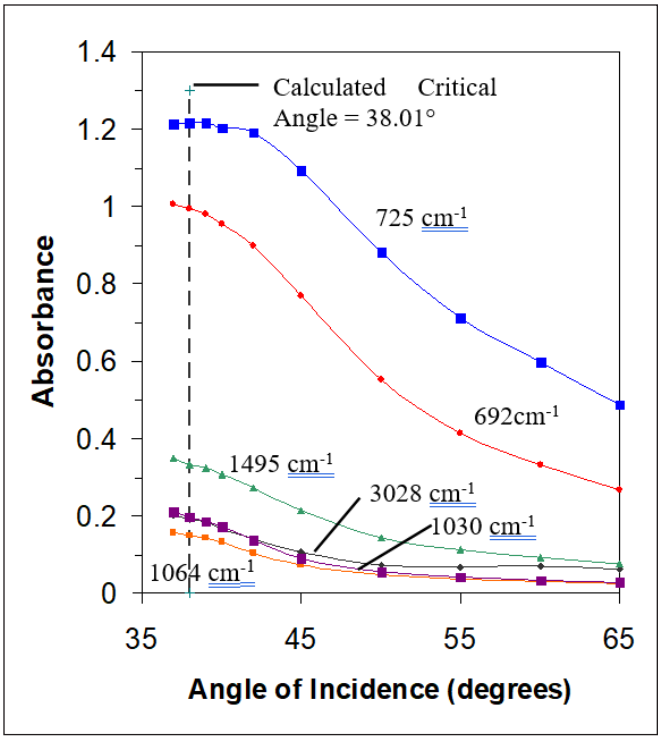

Figure 5. Absorbance vs. angle of incidence for toluene at six absorbance maximum wavelengths without accessory aperture.

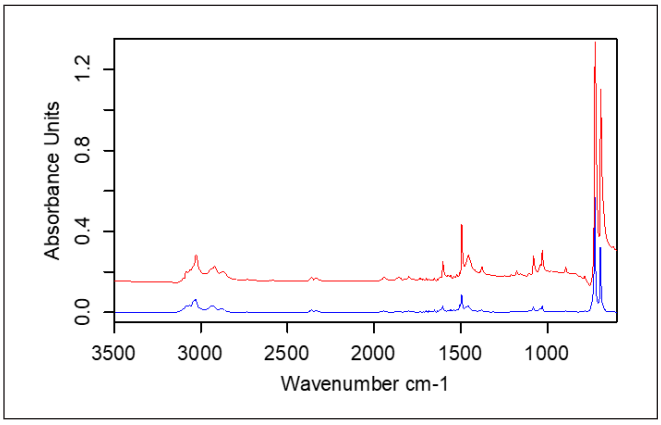

Figure 6. Distorted spectrum of toluene at 39 degrees (top) compared to undistorted spectrum of toluene at 60 degrees (bottom).

at 2000cm^{-1} (5 microns), 2.4295 for ZnSe[2] and 4.0163 for Ge,[3] are used.

Toluene, with a refractive index of 1.4961,[4] is used as the sample in this study. The critical angle, using ZnSe as the ATR material, is 38.010°. The critical angle, using Germanium as the ATR material is 21.870°. Air, used as the sample for the background spectra, has a refractive index of 1.0000. In these cases, the critical angles are 24.306° using ZnSe and 14.417° using Ge, much less than the critical angles with the higher refractive index toluene sample.

Depth of Penetration

The depth of penetration, d_p, defined as the distance required for the electric field amplitude to fall 1/e of its value at the surface,[5] is given by

$$d_p = \frac{W/n_1}{2\pi\left[\sin^2 A - \left(n_2/n_1\right)^2\right]^{1/2}} \qquad (2)$$

where W is the wavelength of light and A is the angle of incidence. The value d_p is an indication of the sensitivity. Using 5 microns as W, and the previously specified refractive indices for ZnSe and toluene, the depth of penetration is plotted versus the angle of incidence in Figure 2. As the critical angle is approached, d_p gets very high. Comparable data for Ge is also shown in the same figure. For any given angle of incidence, the depth of penetration for Ge is much less than that of ZnSe, due to the higher refractive index of Germanium.

EXPERIMENTAL

All spectra were taken with a Thermo/Nicolet Nexus™ 670 spectrometer equipped with a DTGS detector and a standard mid-IR beamsplitter and using Thermo/Nicolet Omnic™ Version 6.1a software. All spectra were run at 4000cm^{-1} to 400cm^{-1}, 64 scans, 4 cm^{-1} resolution, and gain equal to 1. The spectrometer aperture was set to 100 for all runs except where noted. A background spectrum (air) was taken

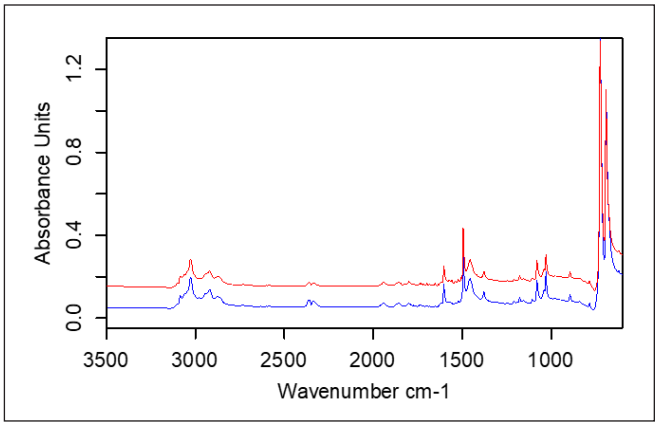

Figure 7. Spectrum of toluene at 39 degrees without (top) and with (bottom) accessory aperture.

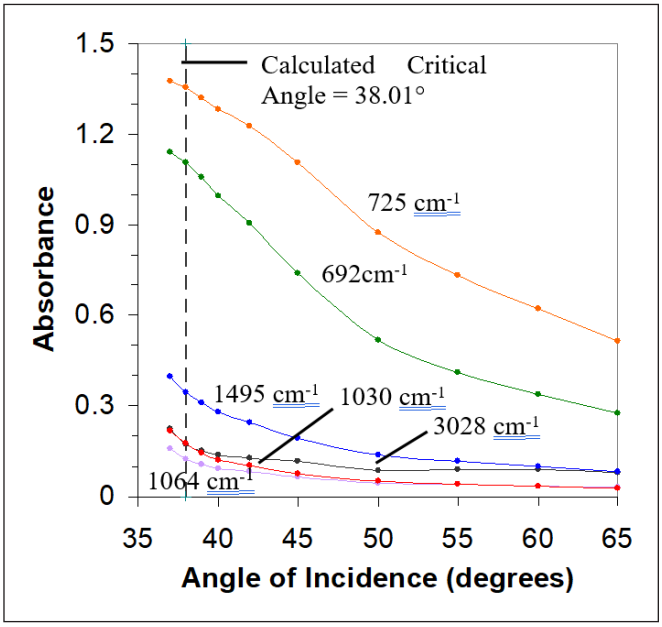

Figure 8. Absorbance vs. angle of incidence for toluene at six absorbance maximum wavelengths with accessory aperture.

prior to each sample spectrum. The purge inputs of the spectrometer and the installed accessory were connected to filtered air (water and CO_2 removed) produced by a Parker Balston unit at 30 SCFH.

A Harrick Seagull™ variable angle reflection accessory was installed in the FTIR spectrometer. See Figure 3. The Seagull accessory allows the angle of incidence to be changed continuously from 5° to 85°. The ATR kit was installed in the accessory along with a Luer-compatible liquid cell. See Figure 4. All runs were taken using a hemispherical ZnSe ATR element, except where noted. A Hamilton Model 1002 2.5ml Luer-tipped syringe was used to inject samples into the liquid cell.

All angles were set in the Seagull™ by first moving the angle several degrees lower than the desired angle and then carefully moving the adjustment continuously higher until the desired angle was reached. This was to assure the consistent removal of any backlash.

Spectrophotometric grade Toluene (Alpha Aesar Stock No. 19376) was used as the samples in all tests, except where noted. A liquid was chosen to avoid any effects due to inadequate contact that might be introduced with solids.

Toluene was the liquid chosen due to particular advantages. It has several peaks of varying intensities over the mid-infrared. It has good solubility in the chosen cleaning solvent, MEK. It has sufficient volatility to assure complete removal prior to taking background spectra. It is not hygroscopic.

The Harrick CristalCalc™ software was used to calculate the depths of penetration used in Figure 2. Transmission spectra were converted to absorbance spectra using the Omnic “Absorb” function. Baseline corrections on the absorbance spectra, where indicated, were performed using the Omnic “Aut Bsln” function. Absorbance peak maxima and associated wavelengths were found using the Omnic “Analyze Find Peaks” function.

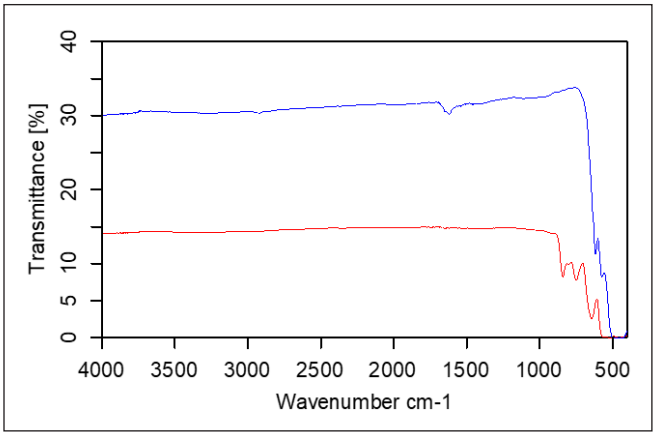

Figure 9. SeagullTM throughput with Zinc Selenide (top) and with Germanium (bottom).

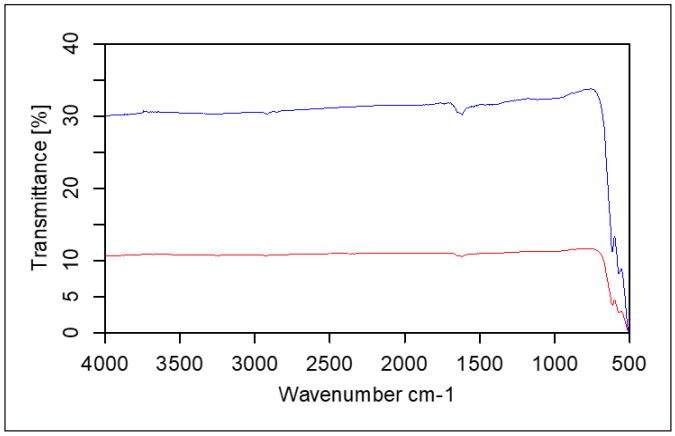

Figure 10. SeagullTM throughput without accessory aperture (top) and with accessory aperture (bottom).

RESULTS

To study the effect of increasing the angle of incidence, three sets of data were acquired. Each set consisted of toluene spectra at the following angles of incidence: 65, 60, 55, 50, 45, 42, 40, 39, 38, and 37 degrees. The averaged absorbance values at six toluene peak maxima (3028cm^{-1}, 1604cm^{-1}, 1495cm^{-1}, 1030cm^{-1}, 725cm^{-1}, and 692cm^{-1}) versus the angle of incidence are given in Figure 5. Baseline correction was applied to spectra obtained for angles of 45 and less. A very small amount of distortion was observed at 45 degrees; significantly more at smaller angles.

The distortion observed was of two types: first, an overall baseline shift toward higher absorbance values; second, a derivative-like distortion in the area of the two strong peaks at 725cm^{-1} and 692cm^{-1}, termed dispersive distortion. These two types can be clearly seen in the spectrum taken at 39 degrees (near the calculated critical angle), shown in Figure 6. A spectrum taken at 60 degrees, shown in the same figure for comparison, has no diortion. The dispersive distortion causes confusion in any baseline correction.

To study the effect of reducing the aperture size on near critical angle distortions, the angle of incidence of the Seagull™ accessory was set to 39 degrees and the aperture of the spectrometer was set from 100 to 40, in steps of 20. No reduction in spectral distortions was observed. A 3mm thick fixed accessory aperture, with a circular opening of 9.5mm diameter, was installed in the Seagull™ accessory in the slide mount used for the optional polarizer. The mount is located on the left side of the accessory. Figure 7 shows two uncorrected absorbance spectra, one without the accessory aperture and one with the aperture. A significant reduction in baseline shift distortion and a small reduction in dispersive distortion are observed for aperture results.

The runs described for the generation of Figure 5 were repeated, but with the accessory aperture installed. The results of these tests are given in Figure 8. For these runs, baseline correction was not required until the angle was reduced to 42 degrees or less. These aperture results show increased absorbance values at the lower angles of incidence

CONCLUSION

The results presented in Figure 5 deviate significantly from expectations based on the theoretical data presented in Figure 2, and may not be accounted for by variations, as a function of wavelength, in the refractive indices of the ATR element, the refractive index of the bulk sample, or the penetration depth.

In Figure 2, the theoretical sensitivity progressively increases as the angle of incidence decreases

until, at the critical angle, the sensitivity is infinite. In Figure 5, the actual sensitivity does start to increase with decreasing angle and then levels off near the calculated critical angle. This pattern in actual sensitivity occurs for high and low absorbance value peaks and at all of the various monitored wavelengths. Distortions start to appear prior to reaching the calculated critical angle. Spectra, although distorted, can still be taken at angles less than the calculated critical angle.

The principal reason for the above observations is optical beam spread in the FTIR spectrometer. This spread is increased by the lensing effect of the ZnSe ATR material. Since there is a variation in angle around the central beam, as the critical angle is approached, a certain percentage of the rays will be less than the critical angle. These rays will exit the ATR element and never reach the detector. An upward shift in the entire absorbance spectrum results. With distortion of this type, the sample causes energy to exit the system. As with an aperture, the overall energy loss results in a decrease in the signal to noise ratio over the entire spectrum. At and below the calculated critical angle, there are still rays at higher angles, and it is these which continue to produce spectra, albeit distorted.

Rays that are near the critical angle have a very large penetration depth. These interact with the fluctuating refractive index of strong sample peaks, producing the dispersive distortion. It is this second type of distortion that makes automatic baseline correction especially problematic.

One method of reducing distortions at any given angle of incidence is to substitute Germanium for Zinc Selenide as the ATR element. The much higher refractive index of Ge results in a lower critical angle for any given sample refractive index. See Figure 1. Germanium, however, does have some disadvantages. First, the sensitivity is decreased for any given angle of incidence. See Figure 2. Second, since reflection losses are greater for the higher refractive index material (in the absence of any antireflection coatings), an ATR accessory with Germanium has a lower throughput than the same accessory with Zinc Selenide. See Figure 9 for the throughputs of the Seagull™ at 45° for these two ATR materials. Third, the greater lensing effect of Ge, due to its higher refractive index, will exacerbate the instrument beam spread even further, when compared with ZnSe. Finally, the same difficulties with spectral distortion encountered with ZnSe near 38° will be encountered with Ge near 22°.

The use of apertures to limit beam spread allows increases in sensitivity to continue as the critical angle is approached. One cannot rely on the aperture built into the FTIR spectrometer, as this component may not be positioned in the optical train to allow restriction of the beam spread. Rather, one must have an independent aperture fixed within the sample compartment or the accessory. The effectiveness of the accessory aperture is shown in Figure 7 which gives uncorrected absorbance spectra of toluene with and without this aperture near the critical angle. The circular aperture cuts out many of the rays that are less than the critical angle, greatly decreasing the baseline distortion described above. Some effect is also observed in the reduction of the dispersive distortion near the two peaks at 725cm^{-1} and 692cm^{-1}. Corrected absorbance baselines of aperture results, therefore, do come closer to zero. Comparison of the baseline corrected absorbances of the two spectra also indicates a sensitivity enhancement for the aperture results. Figure 8 then shows the results of the same runs done for Figure 5, but this time with the accessory aperture in place. Sensitivity enhancement is indicated at angles near the calculated critical angle, especially for the four smaller peaks at 3028cm^{-1}, 1604cm^{-1}, 1495cm^{-1}, and 1030cm^{-1}. Furthermore, the slopes of the four associated curves promise fairly higher sensitivity at lower angles than those tested.

As with the use of Ge, the use of apertures reduces throughput. See Figure 10 for the throughputs at 45° with and without the accessory aperture installed in

the Seagull, using ZnSe as the ATR material. A more efficient aperture could be constructed with a half-moon opening, rather than a full circular opening. This new aperture would block out only the lower angled rays. One can speculate that, with the advent of tunable mid-IR lasers[6] in commercially available spectrometers, true "HyperATR" spectroscopy near the critical angle will be possible. With no beam spread, the critical angle could safely be approached without resort to apertures and their deleterious throughput losses. Mechanical stability would have to be a key feature of such systems, as small changes in the angle of incidence would introduce large absorbance changes.

A pure liquid was chosen as the most convenient sample. The same conclusions would hold for solids and solutions. In fact, detection of trace solutes may become a major application. The use of solutions, however, can introduce nonlinearities due to the association of dissolved species at higher concentrations.[7]

The major emphasis has been to explore practical means to increase sensitivity for measurements of uniform bulk samples. One practical advantage would be to boost sensitivity in detection of the CH stretch, an important organic marker, occurring around $3000cm^{-1}$.[8] As the sensitivity in ATR spectroscopy is proportional to wavelength, the CH stretch peak is typically much weaker than the corresponding peak acquired with transmission spectroscopy. It should be noted however, that there are instances when the sensitivity may be too high. For quantitative analysis, peak maxima should be in the 0.2A to 0.7A range.[9] If peaks have higher absorbances, then the angle of incidence can be increased or Germanium can be substituted for Zinc Selenide.

Alternate means exist for increasing the sensitivity besides variable angle single reflection ATR spectroscopy. By using transmission spectroscopy, the pathlength can be, at least theoretically, increased indefinitely, with an incumbent increase in absorbance values. This approach, however, could prove very problematic for solids and inconvenient for many liquids when compared to the use of ATR spectroscopy. The use of multiple reflection ATR spectroscopy is a common approach to increasing sensitivity. This technique works well for liquids when the sensitivity (proportional to the number of reflections) is well matched to the sample. However, if a number of different samples are to be analyzed, the fixed number of reflections typical of multiple reflection ATR accessories, will not adapt. The use of multiple reflection ATR is limited, when it comes to solids, as hard or curved samples require that the force applied to the sample be exerted over a very small area.

FUTURE WORK

Theory

A clearer explanation for the general nonconformance of the plots shown in Figures 5 and 8 with the expectations of Figure 2 is required. One possible explanation is that, with the beam spread of the FTIR spectrometer, there is, even with the use of an accessory aperture, a significant portion of the rays that are at larger incident angles. These rays serve to reduce the reported absorbance. Rays that are less than the critical angle exit the system and to not add to or subtract from the baseline corrected absorbance values.

A clearer explanation for the S-shaped curves shown in Figure 5 is also required. Detector non-linearity associated with the loss of energy from sub-critical rays is a possible explanation. The fact that without the aperture, many higher angle rays are allowed to contribute, decreasing the overall absorbance, may also be part of the solution. Other effects complicate any explanation. For example, rays closer to the central ray may have a higher intensity than those in the periphery. Also, the beam does not focus to a point, but rather to a spot approximately 6mm in diameter in the open sample compartment.

Equipment and Sample Selection

A variable diameter aperture, with the option of a half-moon opening, is a high priority. The use of an additional pure organic liquid, without the intense

peaks of toluene, would shed additional light on the effects of dispersive distortion on baseline corrections and on possible detector non-linearity due to overall high absorbances. The present liquid cell has a depth of 1.3mm. This should be checked and increased, if necessary. The ATR holder bracket should be equipped with captive screws and ATR retainer brackets to facilitate repetitive cleaning in preparation for new samples.

Procedures

The procedure should include angles well below 37°. A method should be developed to change the angle reproducibly in increments less than one degree near the calculated critical angle.

REFERENCES

1. F.W. Sears and M.W. Zemansky, University Physics Part 2, Addison-Wesley, Reading, 3rd ed. (1965).
2. Crystran Ltd, Dorset, UK (2006), www.crystran.co.uk.
3. S.S. Ballard, K.A. McCarthy, and W.L. Wolfe, Optical Materials for Infrared Instrumentation, University of Michigan Willow Run Laboratories, Ann Arbor (1959).
4. Handbook of Chemistry and Physics, Chemical Rubber Co., Cleveland, 47th ed. (1966).
5. N.J. Harrick, Internal Reflection Spectroscopy, Harrick Scientific Corporation, Ossining (1987).
6. Boston Electronics, Brookline, MA (2006), www.boselec.com.
7. A.I. Vogel, A Text Book of Quantitative Inorganic Analysis, John Wiley, 3rd ed., New York (1961).
8. N.B. Colthup, L.H. Daly, and S.E. Wiberly, Introduction to Infrared and Raman Spectroscopy, Academic Press, 2nd ed., New York (1975).
9. W.J. Blaedel and V.W. Meloche, Elementary Quantitative Analysis, Harper and Row, 2nd ed., New York (1963).